Seasonal variation and release of soluble reactive phosphorus in an agricultural upland headwater in central Germany

Michael Rode[1,2], Jörg Tittel[3], Frido Reinstorf[4], Michael Schubert[5], Kay Knöller[6], Benjamin Gilfedder[7], Florian Merensky-Pöhlein[4], Andreas Musolff[8]

[1]Department Aquatic Ecosystem Analysis, UFZ - Helmholtz-Centre for Environmental Research, Brückstr. 3a, 39114 Magdeburg, Germany

[2]Institute of Environmental Science and Geography, University of Potsdam, Potsdam-Golm, Germany

[3]Department of Lake Research, UFZ - Helmholtz-Centre for Environmental Research Brückstr. 3a, 39114 Magdeburg, Germany (ORCID: 0000-0003-1151-1909)

[4]Department for Water, Environment, Construction and Safety, Magdeburg-Stendal University of Applied Sciences, Breitscheidstr. 2, 39114 Magdeburg, Germany

[5]Department Catchment Hydrology,UFZ - Helmholtz Centre for Environmental Research, Permoserstr. 15, 04318 Leipzig, Germany

[6]Department Catchment Hydrology UFZ - Helmholtz Centre for Environmental Research, Theodor-Lieser-Str. 4, 06120 Halle, Germany

[7]University of Bayreuth, Universitätsstraße 30, 95447 Bayreuth, Germany

[8] Department of Hydrogeology, UFZ - Helmholtz-Centre for Environmental Research GmbH, Leipzig, Germany

Correspondence to: Michael Rode (michael.rode@ufz.de)

Abstract. Soluble reactive phosphorus concentrations (SRP) in agricultural headwaters can display pronounced seasonal variability at low flow, with the highest concentrations occurring in summer. These SRP concentrations often exceed eutrophication levels but their main sources, spatial distribution, and temporal dynamics are often unknown. The purpose of this study is therefore to differentiate between potential SRP losses and releases from soil drainage, anoxic riparian wetlands and stream sediments in an agricultural headwater. To identify the dominant SRP sources we carried out three longitudinal stream sampling campaigns on SRP fluxes. We used salt dilution tests and natural ^{222}Rn to determine water fluxes in different sections of the stream, and carried out specific sampling for SRP, iron and ^{14}C-DOC to examine possible redox-mediated mobilization from riparian wetlands and stream sediments. The results indicate that a single short section in the upper headwater reach was responsible for most SRP losses to the stream. Analysis of samples taken under summer low flow conditions revealed that the stream-water SRP concentrations, fraction of SRP within dissolved P (DP) and DOC radiocarbon ages matched those in the groundwater entering the gaining section. We argue that the seasonal variation of SRP concentrations was mainly caused by variations in the proportion of groundwater present in the streamflow, and was thus highest during summer low flow periods. Stream-sediment pore water showed evidence of reductive mobilization of SRP but the exchange fluxes were probably too small to contribute substantially to SRP stream concentrations. Examination of the combined results of this campaign and previous monitoring confirms that groundwater is also the main long-term contributor of SRP at low flow and that seepage from agricultural phosphorous is largely buffered in the soil zone. In this headwater, stream SRP loading

during low flow is therefore mainly geogenic, while agricultural sources play only a minor role in SRP loading, with the dominant SRP sources being the local Paleozoic greywacke and Devonian shale. Because it is also possible for similar seasonal SRP dilution patterns to be generated by enhanced mobilization in riparian zones or wastewater inputs, precise knowledge of the different input pathways is important to the choice of effective management measures.

1 Introduction

Land-to-water diffuse phosphorus emissions caused by intensive agricultural land use are a major cause of eutrophication in streams and rivers (Bol et al. 2018). Phosphorus losses from headwater catchments are the result of integrated hydrological and biogeochemical processes occurring within the drainage area and in the stream (Bormann and Likens 1967, Bernal et al. 2014). Such headwater P transport processes can exhibit high spatio-temporal variability and are controlled by landscape properties. This high variability is especially well-described for particulate P losses (Bechmann et al. 2008, Bol et al. 2018). However, recent studies suggest that dissolved and colloidal P mobilization from agricultural land can also lead to high seasonal variation in soluble reactive phosphorus (SRP) concentrations in headwater streams (Bol et al. 2018). This variability in seasonal P concentrations is possibly of greater importance than previously assumed (Dupas et al. 2018) and can be related to the change of shares of different P sources within the year. SRP mobilisation can occur in various headwater compartments, comprising a) soils via preferential flow in soils and tile drainage, b) riparian wetland in connection with anoxic conditions and a reductive dissolution of Fe oxyhydroxides (Tittel et al. 2022), c) stream sediments via the same reductive process (Kleinman et al. 2003, Gu et al. 2017, Smolders et al. 2017), and d) groundwater systems (Brookfield et al. 2021).

The leaching of dissolved P from soils has been linked to surface-soil P desorption (McDowell and Sharpley 2001) and the application of fertilizer (Chardon et al. 2007). The dominant form of subsurface transport is undoubtedly preferential flow through soil macropores (Simard et al., 2000). Artificial drainage provides a lateral short cut between subsurface macropores and surface water and can therefor lead to environmentally important P losses (Dils and Heathwaite, 1999). In addition, factors such as soil P sorption saturation (P_{sat}) and oxidation-reduction cycles can greatly increase P mobility through soils (Behrendt and Boekhold, 1993; Heckrath et al., 1995). The lateral transport of P is mostly induced by artificial drainage, but also occurs in association with particular soil characteristics, e. g. sandy soils (Kleinman et al. 2009).

The hydrological variability of riparian wetlands has also been widely shown to influence SRP mobilization via redox conditions in soils. The high water table and low-velocity flow episodes that usually develop in riparian wetlands during the wet season can create anoxic conditions. This can lead to the reductive dissolution of Fe (hydr)oxides (Jeanneau et al., 2014; Knorr, 2013) and hence to solubilization of the P previously adsorbed or co-precipitated onto/within these Fe (hydr)oxides (Zak and Gelbrecht, 2007). Similar findings have been recorded for upland headwater catchments, with increased SRP mobilization via redox processes during periods when groundwater levels are high (Dupas et al. 2017). It is assumed that these temperature-dependent biogeochemical processes could lead to P release into rivers during the summer low flow period when NO_3^+ is denitrified and thus missing as a redox buffer for the reductive mobilization of Fe oxides (Musolff et al. 2017, Dupas et al. 2018).

Stream sediments have potential to remove or release P to the stream water during summer low flow conditions (Simpson et al. 2021). When streams are mainly fed by groundwater, P reactions in the hyporheic zone may control the release of P. Data suggest that anoxic conditions can cause the release of sediment P in streams (Simpson et al. 2021). The highest seasonal concentrations of SRP (i.e., mainly monomeric PO4) are often found in summer and during low flow, and are higher in lowland than in upland rivers (Bowes et al. 2003). Molybdate reactive P redox-mediated release from river sediments has been identified in lowland rivers during summer anoxia (Smolders et al., 2017). This mobilization of P from sediments to the water column was found to be related to the molar P/Fe ratio in stream sediments. The authors suggested that the temporal and spatial variability of soluble P in the water body of lowland rivers was mainly related to internal loading, i.e., to the legacy P in the sediment and not to the corresponding variability in emission and dilution rates (Smolders et al. 2017).

Groundwater systems can be important sources for the mobilization and transport of P to surface waters. The P concentration in groundwater depends on the geology and long-term land use pattern in the catchment (Brookfield et al. 2020). Long-term agricultural activities can result in soil P concentrations exceeding the soil sorption capacity, which under right conditions can be released into the groundwater system in dissolved form (Brookfield et al. 2020, Haygarth et al. 2014). In addition to this accumulation of P in groundwater through anthropogenic activities, the extent of water-rock interaction can also impact the P concentration in groundwater. An important factor is the contact time of groundwater with the surrounding media, and slower groundwater flows can lead to more interactions between water, rock and microbes. For example, chemical weathering can affect the sorption of P onto aquifer minerals, where the sorption ability of P can decrease with increasing pH (Cornell and Schwertmann 2003).

A recent comparative study in forest and agricultural headwaters revealed that the highest levels of seasonal SRP occurred in headwater streams featuring riparian wetlands or high groundwater levels in the near stream zone (Dupas et al. 2017). The agricultural Schäfertal catchment is a typical headwater of the central German lower-mountain hard-rock area. Until now it has been unclear which P sources and transfer pathways are responsible for the distinct seasonal pattern of winter lows and summer highs in SRP level, and evidence is lacking on the dominant P transfer. Furthermore, it is not clear how land use (e.g. P status) might impact baseline SRP concentrations, nor which factors control SRP mobilization (e.g. groundwater heads, land use, temperature, redox processes, P status of riparian zones etc.). Analysis of these controlling factors would enable identification of the sources of SRP in a characteristic hard-rock agricultural catchment in a lower mountain range.

The objectives of the present study of SRP release in headwater during baseflow condition are: a) to identify the main pathways for SRP transfer into the stream water (transfer from hillslopes, redox-controlled delivery from riparian wetlands, release from stream sediment); b) to localise the major source areas of SRP within the catchment; and c) to explain the mechanisms leading to the development of characteristic seasonal SRP concentrations.

This study aims to identify spatially-localised gaining- and losing water fluxes along the Schäfertal stream using salt tracer injections and longitudinal measurements of the ^{222}Rn activity concentration in the stream water. By combining these spatially distributed water fluxes with longitudinal water-quality measurements, it was possible to quantify land-to-water SRP fluxes along the whole stream. To identify the SRP release processes, we conducted additional radiocarbon, DOC and Fe

105 measurements in gaining groundwater and in the streambed sediments for comparison with the stream-water signature. Combined compartment-specific measurement campaigns under summer and winter low-flow conditions enabled us to evaluate the seasonal behaviour of SRP transport in the study headwater.

2 Material and methods

2.1 Study site

110 The Schäfertal watershed is an agricultural headwater catchment (1.44 km^2, Figure 1), located in the lower Harz Mountains in central Germany. Elevation ranges from 391 to 474 m. The north- and south-facing hillslopes, with an average slope of 11°, are intensively cultivated (crop rotation: winter wheat, triticale, rapeseed, winter wheat); mineral-fertilizer application levels were between 60 kg (rapeseed) and 148 kg (winter wheat) N ha^{-1} y^{-1}, and between 11 and 14 kg P ha^{-1} y^{-1} (LLFG 2021, Kistner et al. 2013). In 2018 the cropping system shifted to organic farming and no more mineral fertilizer was applied. The mid-
115 catchment valley bottom is dominated by grassland with drainage channels; the upstream hilltop is occupied by sparse forest (Figure 1).

The underlying Paleozoic greywacke and Devonian shale are covered by periglacial layers with different fractions of loess and rock fragments, resulting in complex geomorphological structures through the soil profile (Kistner et al., 2013). The hillslope soils (Altermann and Mautschke, 1970; Graeff et al., 2009) exhibit relatively high porosity and hydraulic conductivity (mean
120 value 9.95 * 10-6 ms^{-1}) in the top soil layer, and lower hydraulic conductivity (mean value 2.31 * 10-7 ms^{-1}) in the base layer at depths below 0.4 m (Graeff et al., 2009). Soil properties ascertained by field soil core sampling are generally homogenous (Schrön et al., 2017), with a certain degree of spatial variability caused by detailed topographic characteristics as slope position, valley bottom and exposition (e.g. those reported in Ollesch et al., 2005; Anis & Rode, 2015). Additionally, there is an extensive network of artificial tile drains throughout the central valley bottom (see Yang et al. 2021). Fluvisols and Gleysols
125 dominate in the valley bottom and are partly drained by the tile drainage network. The arable hillslope soils are Gleyic Cambisols and Luvisols, and a small area of forest soils made up of Rankers and Cambisols is found at the top of the catchment (Figure 1) (Yang et al. 2021). It can be assumed that aquifer thickness ranges from 2 m at the top of the hillslopes to 5 m at the valley bottom (2.4 m on average), based on the dominance of Gleysols and Luvisols toward the valley bottom (Yang et al. 2018). The stream itself has a length of 1747 and a slope of 2 %, with a mean discharge of 0.33 mm d-1 (5.5 L s^{-1}). The stream
130 has a mean width of 0.4 m and a depth of 0.05 m. The substrate consists of fine and mid-granular sand fraction. It is an open canopy stream with high light availability, the forest area of 3 % of the catchment area is not located along the stream.

Previous research has shown mean soil TP content in the top soil layer (3-5cm) to be 916 mgP kg^{-1} while water-soluble phosphorus (WSP) content is 13.1 mg P kg^{-1}, indicating a strong influence from fertilizer use. Degree of phosphorus saturation (DPS) is 31.7% (Kistner et al. 2013). It can be assumed that the TP concentration will change only slightly over time (Little et
135 al. 2007) while modelling has shown that temporal variation in WSP concentrations can be high, caused by fertilizer application and crop uptake (Kistner et al. 2013). Calculated short-term declines of DSP in the top soil layer (upper 2cm of soil) can be

explained by rainfall events. This suggests a transport of soluble P compounds to deeper layers (Kistner et al. 2013). Top-soil WSP concentrations also display high spatial variability, from 2.3 to 37.6 mg P kg^{-1} (Kistner et al. 2013). The recorded means for soil organic carbon content and pH in the top soil layer are 21.3 g kg-1 and 6.39 respectively (Kistner et al. 2013). DOC
140   concentration in soil pore water ranges between 1.2 and 62.6 mg L^{-1} (Ackermann, 2016).

Due to its location in the eastern lee of the Upper Harz mountains, the catchment sits in a rain shadow of the Brocken mountain and therefore has a relatively low average annual precipitation of about 629 mm a-1 (1991-2020). Precipitation is relatively evenly distributed over the year, with slightly higher precipitation values in summer. The discharge regime of the Schäfertal stream, however, is dominated by higher discharges in winter, mainly due to snowmelt, and low flow periods in summer
145   (Figure 2). The influence of earlier mining activities on the flow regime and groundwater levels ceased with the mining activities in the beginning of the 1990s, and pre-mining hydrological conditions have returned. In summer, the stream regularly dries up in the area near the source, while it is perennial in the lower sections. The dynamics of groundwater levels near the wetland in the central part of the catchment show a significant decrease brought about by the relative strong drought

150
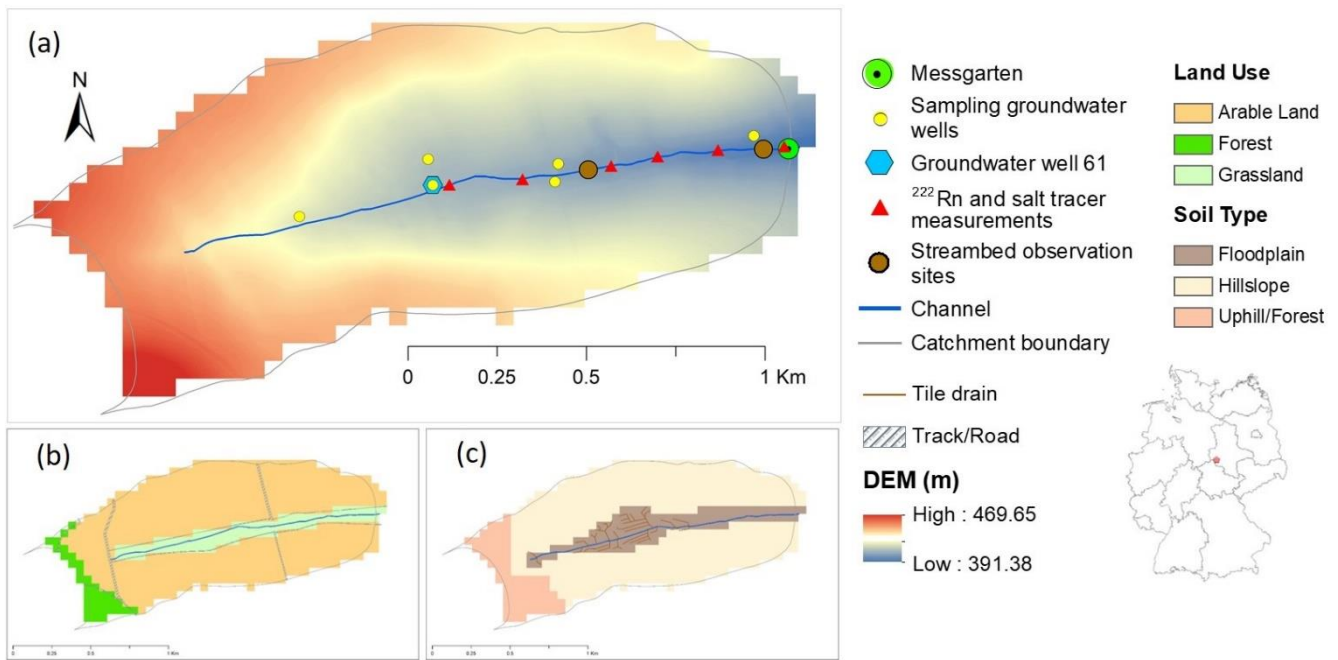
Figure 1. The Schäfertal catchment and monitoring locations used by Yang et al. (2021), showing (a) digital elevation model (DEM) and monitoring sites with sampled groundwater wells, (b) Land use types, and (c) soil types and the tile drain network. A V-notch weir is installed in the Messgarten climate station for discharge measuring and stream water sampling (adapted
155   from Yang et al., 2021)

in 2018-2019 (well 61, see Figure 1, period 2010-2021, Supplement). An isotope-tracer aided modelling study has shown that under these drought conditions modelled stream runoff from deeper, older storages increased significantly after a particularly wet season, resulting in a sharp increase in stream water age (Yang et al. 2021). Earlier long-term water quality measurements

160   at the catchment outlet (1999-2010) reveal discharge NO3-N concentration to be between 0.11 and 11 mg L-1 (mean = 4.37 mg L^{-1}), DOC concentration between 1.7 and 12.6 mg L^{-1} (mean = 4.23 mgL^{-1}), SRP between 0.002 and 0.16 mg L-1 (mean = 0.025 mg L^{-1}), and TP concentrations between 0.009-0.33 mg L^{-1} (mean = 0.067 mg L^{-1}). Baseflow stream-concentration data show clear seasonal variations in amplitude with N03 highs in winter and DOC and SRP highs in summer (Dupas et al. 2017).

2.2 Low flow measurement campaigns

165   Measurement campaigns took place after snowmelt in January 2019 during a period of slightly elevated discharge and groundwater levels, and in September 2019 and 2020 during prolonged periods of low flow and low groundwater levels. These campaigns comprised in-stream salt tracer dilution tests and ^{222}Rn measurements in order to analyze lateral inflows to the stream, and water quality measurements to characterize stream water, riparian groundwater and stream sediment properties.. Meteorological conditions for all campaigns were characterized by comparatively low rainfall in the preceding days (Figure

170   2). The groundwater levels (m below surface) in the sampling period ranged between 0.5 and 1.1 m. Relating to the 3 sampling campaigns groundwater levels were at 0.65 m (Jan. 2019), 1.0 m (Sep. 2019) and 0.85 m (Sep. 2020) below surface (see Figure S, Supplement).
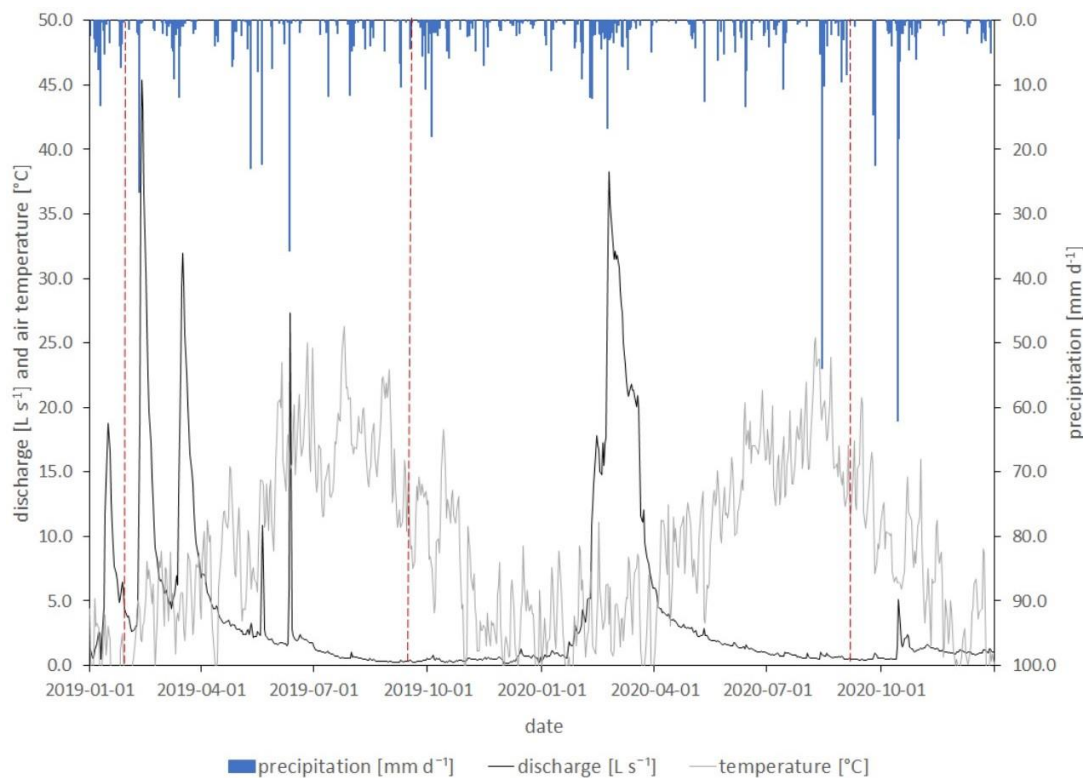
Figure 2: Daily precipitation (mm d^{-1}), daily average discharge (L s^{-1}), daily average air temperature (°C) for the Schäfertal stream during the measurement campaign period. Red dotted lines mark campaign dates.

2.2.1 Lateral inflows to the stream

2.2.1.1 Water balance of stream sections measured by tracer dilution tests

Consecutive salt tracer dilution tests were applied to quantify gross gains, gross losses and net change following Payn et al. (2009). The tracer tests were performed in January 2019, September 2019 and September 2020 at six locations defining five stream sections with lengths between 130 and 250 m. The observation point furthest downstream was located a short distance (100 m) above the gauging station. The total length of the stream sections studied was 955 m. The sodium chloride tracer was prepared in the lab and diluted in 7 l of stream water prior to injection. In the two 2019 campaigns, 500 g of tracer was used for each injection while in the 2020 summer campaign, 100 g of tracer was used. The tracer was injected 10 m upstream of each observation point, giving a mixing length of 20 to 30 times the stream's width. Tracer breakthrough was measured at 5-second intervals using individual in situ conductance loggers (Eijkelkamp CTD-Divers) fixed in a central position of the stream. The tracer was injected working consecutively upstream from the observation point downstream with a time interval of 30 min to ensure that the breakthrough curves of consecutive injections did not overlap. The measured time series for

specific conductance were converted to sodium chloride concentrations using a linear regression (with the intercept fixed at zero) for each individual data logger based on four data points with known sodium chloride concentrations (measured in the lab). The background specific conductance was subtracted from the time series prior to conversion. For each tracer breakthrough concentration [mg L^{-1}], the time series was summed up to mass flux [mg L^{-1} s^{-1}]. A known injected tracer mass [mg], makes it possible to derive discharge [L s^{-1}]. Following Payn et al. (2009), we quantified breakthrough of the injection at each observation point in relation to the breakthrough of the injection at the observation point immediately upstream, assuming that the net change in discharge is the sum of gross gains and gross losses along the stream. The net change for a given section is calculated as the difference between upstream and downstream discharge measurements. Gross loss for each section is derived at the downstream observation points from mass recovery analysis of the upstream injected tracer and upstream discharge. Gross gain for each section is derived from the difference between net change and gross loss. Note that, in the 2019 summer campaign, it was not possible to measure upstream injection breakthrough for the uppermost two sections because flow velocity was too low for breakthrough to be measured in the allotted time. In summer 2020, this was the case for the uppermost section only. Here, only net changes could be quantified.

2.2.1.2 Groundwater discharge investigated by Radon (^{222}Rn) measurements

Natural radon (^{222}Rn) activity concentrations in the stream water were used in addition to the salt tracer investigations to provide insight into both the spatial distribution and the quantity of groundwater discharge into the Schäfertal stream along the investigated stream section. Radon is an excellent tracer for investigating groundwater-surface water interaction (Petermann et al. 2018). Longitudinal stream radon measurements allow (i) localization of groundwater discharge zones and (ii) calculation of radon mass balances within defined sections of the stream, enabling groundwater discharge into the stream to be quantified. A crucial parameter for this method is the rate of radon degassing from the stream, which is primarily dependent on the stream turbulence, i.e., on stream geometry, streambed roughness and stream flow velocity (Genereux and Hemond 1992, Raymond et al. 2012). A number of experimental and empirical methods are available to estimate radon degassing from a stream. A detailed discussion of the approach applied in the study is provided in Schubert et al. (2020). Furthermore, Raymond et al. (2012) has published a comprehensive review of scaling gas transfer velocity in streams and small rivers. Radon mapping along the Schäfertal stream was carried out during the low-flow measurement campaigns in January 2019 and September 2020. During each campaign, stream-water samples were taken from six locations distributed (roughly) equidistantly along the study reach of the stream, thus subdividing the study reach into five sub-sections (cf. Figure 6). The radon sampling points were identical to the salt traces measurement points. To determine the radon groundwater endmember, water samples were taken from three groundwater wells located adjacent to the stream and from two subsurface agricultural drains that discharge into the stream within the section located furthest upstream. Radon measurements were carried out on-site immediately after sampling by means of a mobile radon-in-air monitor (RAD7) as described by Schubert et al. (2006). Based on the resultant radon data (i.e., on the radon mass balances for the five sub-sections) groundwater discharge localization and quantification were performed using the implicit finite element model FINIFLUX, which is described in detail in Frei and Gilfedder (2015).

FINIFLUX numerically solves the mass balance equation for in-stream ^{222}Rn at the reach scale by using a Petrov-Galerkin Finite Element scheme based on on-site radon measurement results. The model input parameters include (i) the length of the investigated sub-section, (ii) its mean width and mean depth, (iii) the discharge of the stream, as well as the ^{222}Rn activities of (iv) the stream water specific for the sub-section and of (v) the overall groundwater endmember. Related to the latter, hyporheic exchange is also allowed for by the model (based on the physical characteristics of the hyporheic zone). Furthermore considered are (vi) a degassing coefficient (specific for the stream sub-section) and (vii) the first order decay constant for ^{222}Rn.

2.2.2   Stream water, groundwater and stream sediments chemistry

Longitudinal water-quality measurements (n=11) were carried out during the three campaigns at intervals of approximately 100 m, starting at the outlet discharge gauging station (in the "Messgarten") using a YSI 610 multiparameter probe (O2, pH, electric conductivity) and a TRIOS ProPS-UV sensor with an optical path length of 2 mm (NO3). Probes were calibrated at the day of measurement. Further details on accuracy, detection limits and standard methods are given in Rode et al. (2016). Additional grab samples were taken for the measurement of SRP and DP using standard methods. The pore size of filters was 0.22 µm. Total (TP) and reactive phosphorus (SRP) were measured using the ammonium molybdate spectrometric method (DIN EN ISO 6878, 2004). Detection limit was 0.005 mgPL-1.

To elucidate SRP concentrations in potential source zones and possible redox-mediated mobilization, SRP and dissolved iron from groundwater wells were measured during the September 2020 campaign. Dissolved Fe concentrations were measured by ICP-OES (Perkin Elmer 7300 DV). The limit for determination was 0.01 mg L^{-1}. Additionally, SRP and dissolved iron were measured in gaining groundwater, streambed pore water and the stream itself. Groundwater samples were taken from six wells near the stream using a peristaltic pump. Streambed pore water samples were taken at two observation points, one located 400 m from the head of the study reach ('upstream station'), and the other located 900 m from the head ('downstream station' or 'outlet'). Gaining groundwater was sampled at the upstream station. Additionally, samples for 14C-DOC were taken from stream water and from stream-sediment leachate from both, the upstream station and outlet as well as from gaining groundwater at the upstream station.

Pore water and gaining groundwater were sampled using PTFE piezometers with a diameter of 10 mm and a screen length of 80 mm. The piezometers were placed in the streambed sediments with the help of a solid metal rod, either at a depth of 7 cm below the streambed surface (pore water), or at the bottom of the sediment at a depth of 15 cm (gaining groundwater). Samples were drawn through a PTFE tube with a syringe and filtered with 0.45 µm cellulose acetate filters on site before being transported in gas-tight flasks without headspace and cooled in the laboratory.

Streambed sediment samples were taken at both stations using a shovel from depths of 5 cm. In the laboratory, 25 g of sediment was slurried with 150 mL of deionized water and incubated for 24 h in an overhead shaker at 20°C in the dark. The pH ranged between 5.0 and 6.1 at the end of incubation. After centrifugation (5250 g, 15 min) the supernatant was filtered (Whatman GF/F, pre-combusted for 4 hours at 500°C) and the DOC in the water samples was processed for radiocarbon analysis as described previously (Tittel et al., 2013). Radiocarbon quantities were analyzed by accelerator mass spectrometry (AMS) at

the Poznan Radiocarbon Laboratory (Poland). The results refer to the oxalic acid II standard and were corrected for fractionation (Stuiver et al., 1977).

3 Results and Discussion

3.1 Observed discharge and stream SRP concentrations

260 During the January 2019 campaign, the stream discharge at the outlet was 5.35 L s^{-1}. By contrast, the summer campaigns were carried out under strong drought conditions and the stream discharge measured at the outlet was only 0.26 L s^{-1} (Sep. 2019) and 0.51 L s^{-1} (Sep. 2020) (see Figure 2). During the two summer campaigns, SRP concentration at the outlet (mean values 0.048 mg P L^{-1} in Sep. 2019 and 0.033 mg P L^{-1} in Sep. 2020) was by a factor of 4 to 8 higher than in the winter campaign (0.009 mg P L^{-1} in Jan 2019). SRP concentrations displayed very constant longitudinal behaviour with a very slight increase

265 downstream from 0.008 mg P L^{-1} to 0.009 in Jan. 2019 (Figure 3). We monitored more pronounced increases in Sep. 2019 from 0.024 mg P L^{-1} to 0.068 mg P L^{-1} and in Sep. 2020 from 0.022 mg P L^{-1} to 0.040 mg P L^{-1}. Dissolved P (DP) was 0.040 mg P L^{-1} higher than SRP during both 2019 campaigns but only 0.001 higher in Sep. 2020. The strongest increase in SRP concentrations was found at a distance of approximately 200 m from the head of the study reach during summer
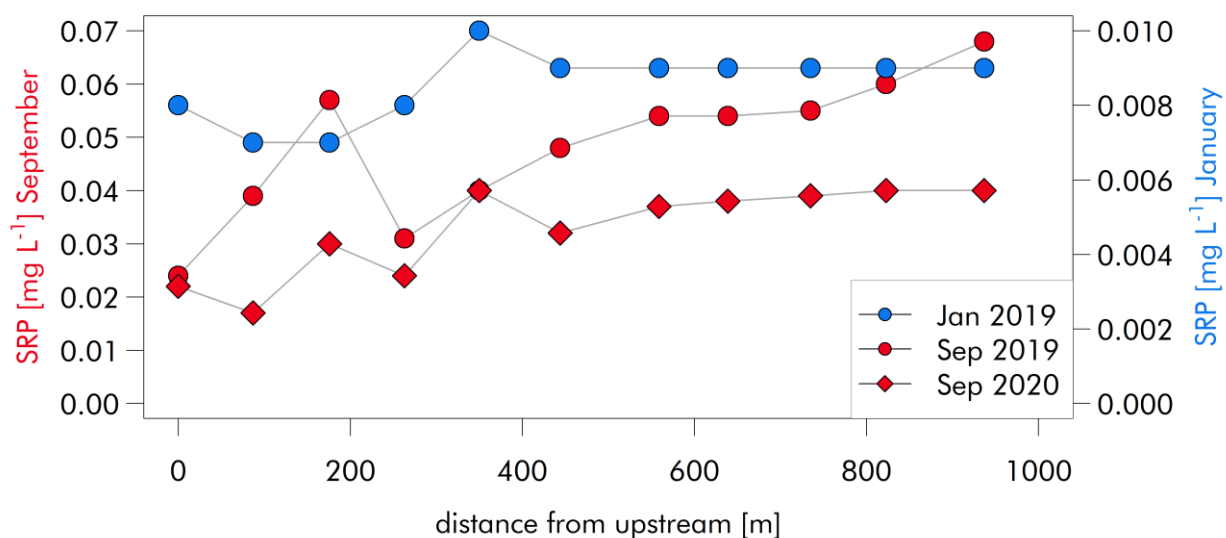
270

Figure 3: Longitudinal SRP concentration profiles for the three measurement campaigns in January 2019 and September 2019 and 2020.

campaigns, whereas the highest concentrations in Jan. 2019 were observed at a location approximately 400 m from the head
275 of the reach (Figure 6). Nitrate concentrations tended to increase from upstream to downstream during both summer campaigns
up to 3.81 mg N L^{-1} (Sep. 2019; mean 3.59 mg N L^{-1}) and 4.48 mg N L^{-1} (Sep.2020; mean 4.50 mg N L^{-1}). A much higher
mean NO3 concentration of 12.7 mg N L^{-1} was recorded during Jan. 2019, indicating high levels of agricultural pollution.

3.2 Observed longitudinal water and SRP fluxes

The salt tracer dilution tests revealed a distinct, non-uniform distribution of discharge gains. In the Jan. 2019 campaign, the
280 two uppermost stream sections for these tests (0 to 460 m) cumulatively gained 44% of the discharge observed at the gauging
station. The three downstream sections did not further increase the discharge, while the lowest stream section in fact
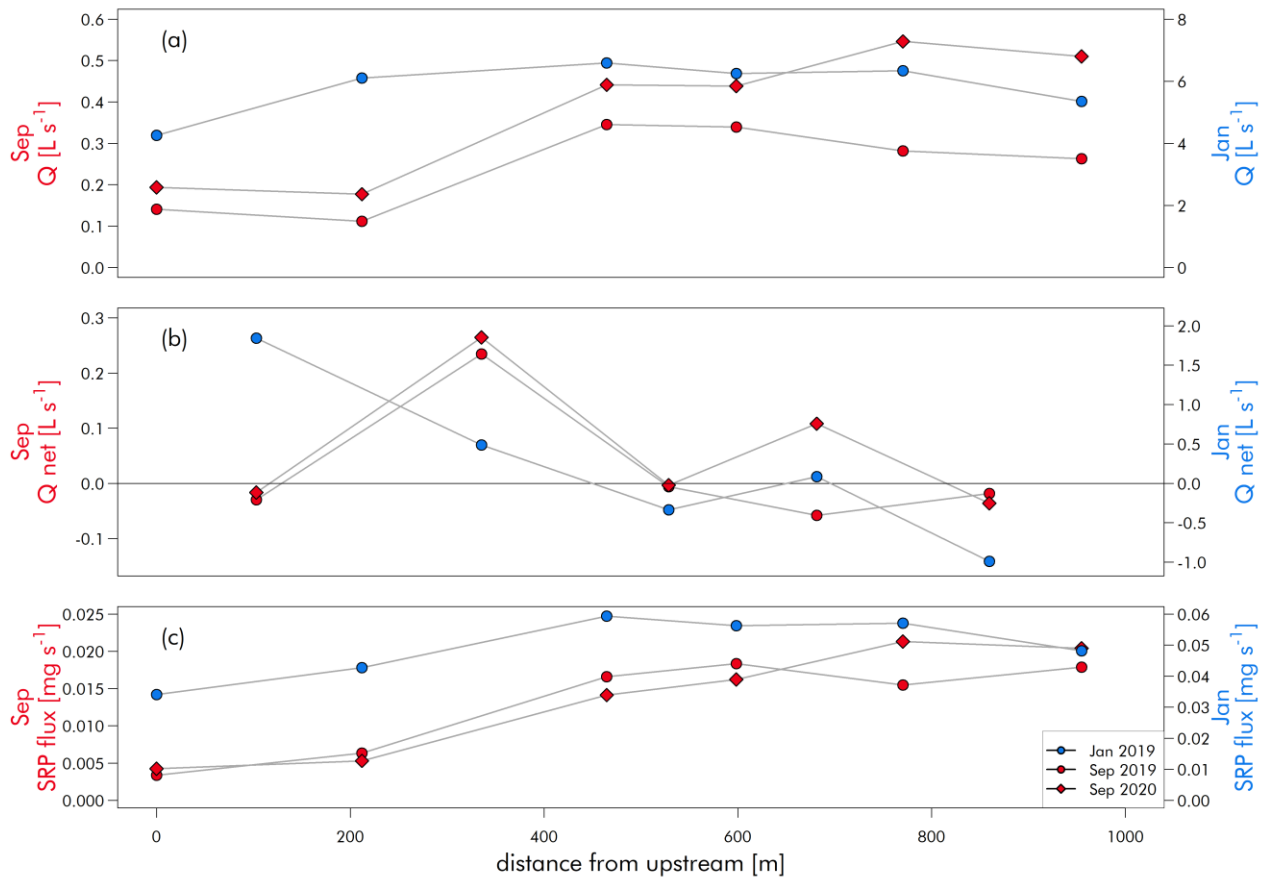
285 **Figure 4:** Net discharge gains and losses, absolute discharge, and total SRP flux along the stream during the three sampling
campaigns.

showed significant losses. In the two September campaigns, a high proportion of the discharge gain occurred in the second section alone (210 m to 460 m from upstream). In this section 52% (2020) to 89% (2019) of the discharge observed at the

290   outlet entered the stream. The sections furthest upstream and downstream had little net change in discharge, and there were small gains in the fourth section in September 2020.

The SRP flux at the outlet in the winter campaign (0.048 mg s-1) was double the flux observed during the two September campaigns (0.018-0.028 mg s^{-1}). The spatial pattern of discharge along the stream largely translated to the pattern observed for SRP flux. In January 2019, the two upstream sections gained 52% of the SRP flux observed at the outlet, while the downstream

295   section lost some water and SRP. In the September campaigns, just one stream section gained 43% (2020) to 57% (2019) of the SRP flux observed at the outlet. In 2020, we observed a further increase in the lowest three sections of 30%, which had not been observed in 2019.

3.3 Groundwater discharge investigated by [222]Rn measurements

The two radon sampling campaigns resulted in almost identical radon concentration distribution patterns along the study reach, with high radon concentrations in the two upstream sub-sections and concentrations declining exponentially at approximately similar rates in the three downstream sub-sections (Figure 5). The radon groundwater endmember (as determined from samples taken from three groundwater wells and two subsurface agricultural drains) amounted to 23.2 ± 1.14 kBqm^{-3}. In the summer campaign, the very low water level at the sampling point furthest upstream made it necessary to dig a small hollow in the streambed sediment for stream-water sampling. This interference with the natural profile of the streambed is highly likely to have resulted in a minor but locally significant preferential groundwater discharge pathway, leading to a radon concentration in this particular sample that can be assumed to be closely representative of pure groundwater. Accordingly, the value detected here was not considered representative of stream water at this location (displayed by a dashed line in Figure 5).

Although the radon distribution patterns of the winter and summer plots are roughly comparable (Figure 5), the concentrations observed during the winter campaign were about 20 times higher than in summer. This general difference is thought to result from the differences in hydrological conditions. The summer campaign was conducted under hydrological strong drought conditions, implying low groundwater levels and low groundwater discharge to the stream. By contrast, the winter campaign was characterized by high groundwater levels generating normal baseflow into the stream.

Groundwater discharge rates were calculated based on the determined radon endmember in groundwater (23.2 ± 1.14 kBq/m³) and the radon in stream water concentrations displayed in Figure 5 using theFINIFLUX model. The results for the five stream sub-sections consistently revealed that the majority of groundwater discharge occurred in the second upstream section. The exponential decrease in radon concentration in the following three downstream sections reveals degassing as the dominant radon sink with little or no contribution from radon sources such as groundwater discharges or hyporheic exchange.

The section-specific quantification of the discharges was more difficult than their localization, due to considerable uncertainties in parameterizing radon degassing for the FINIFLUX model. The uncertainties of our FINIFLUX model results are mainly correlated to the uncertainty of the applied degassing coefficient (for a detailed discussion see Schubert et al. 2020). For estimating how sensitive our modelled groundwater discharge rates are to the applied degassing coefficient, we calculated a range of uncertainties exemplarily for the winter campaign (with a modelled cumulative groundwater discharge rate of 0.75 L s^{-1}). For this purpose, we increased/decreased the degassing coefficient applied in FINIFLUX stepwise up to ±25 % and run several individual model calculations. The resulting cumulative groundwater discharge rates ranged from 0.42 to 1.13 l s^{-1} (mean 0.75 L s^{-1}) with the higher discharge rates associated with larger values for the degassing coefficient. Hence, a ±25 % uncertainty in the applied degassing coefficient corresponds to a relative uncertainty in the modelled groundwater discharge ranging between ca. -45 and +50 %.
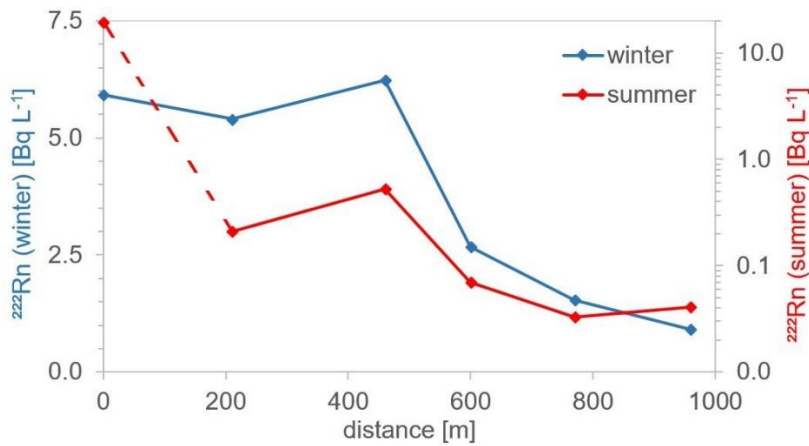
Figure 5: [222]Radon concentration patterns along the stream sections during winter (Jan 2019) and summer (Sept. 2020) campaigns; the dashed line indicates that the most upstream "summer" sample cannot be considered representative of stream water (see text above)
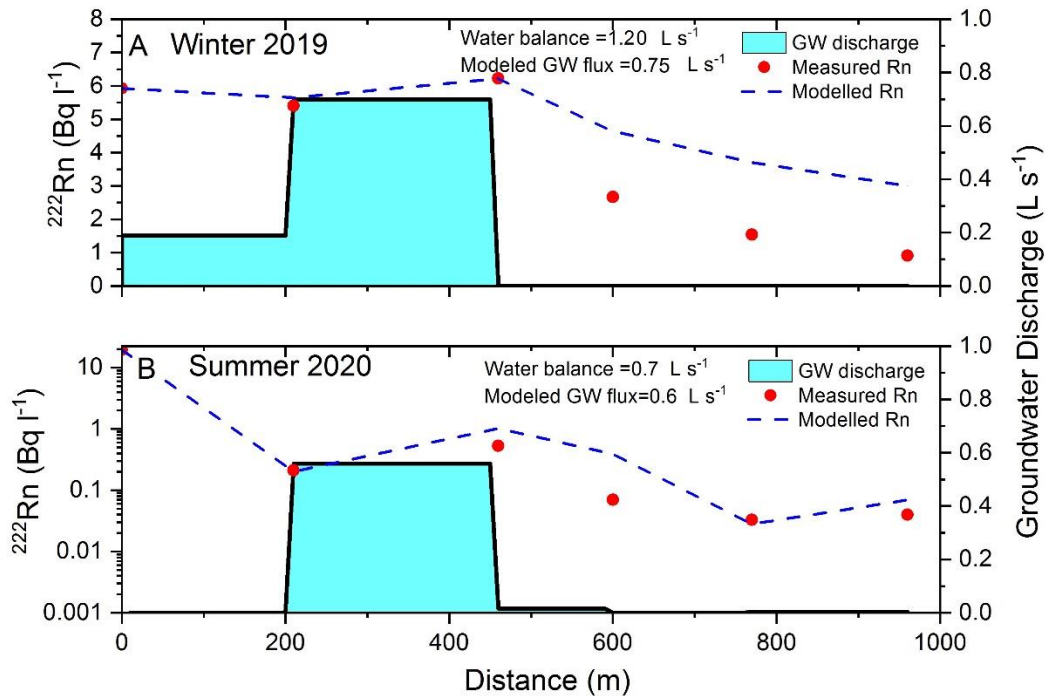
Figure 6: [222]Radon concentrations in the stream water (measured and modelled) and groundwater discharge levels during A the winter (Jan. 2019) campaign and B the summer (Sep. 2020) campaign; note that the most upstream "summer" sample was not considered representative of stream water (see Figure 5)

For the winter campaign, the radon-based quantitative results for cumulative groundwater discharge within the study reach gave a value of about 0.7 L s^{-1} (Figure 6a). This suggests that about 60 % of all water entering the stream (1.2 L s^{-1}) was groundwater.

During the summer 2020 campaign low stream discharge (0.51 L s^{-1}) lead to a very shallow water level (only centimetres) and a very low flow velocity for the stream water (around 0.07 m s^{-1}). This resulted in intense radon degassing from the stream along its flow path. Even though the FINIFLUX model could allow for this high radon loss by degassing, the modelling of groundwater discharge quantities during the summer campaign proved more difficult than for the winter campaign. The most plausible cumulative groundwater discharge rate calculated on the basis of the radon measurement data is 0.6 L s^{-1} (Figure 6b). This suggests that nearly 100 % of the water gained by the stream during the summer campaign along the study reach was derived from groundwater.

3.4 Assessing potential sources of SRP in summer baseflow (Sep. 2020)

Under summer low-flow conditions in September 2020, we conducted a systematic survey of potential sources for the SRP entering the stream: streambed sediments and shallow-sediment pore water were sampled at the upper observation point of the section with the highest gains (400 m from the top of the study reach) and at the downstream discharge gauging station located at the outlet. Further samples of groundwater were taken from the surrounding wells and directly from the deeper part of the streambed at the upstream station. SRP, Fe, DOC and NH4 concentrations, ratio of SRP/DOP, where we define DOP as DP minus SRP, and radiocarbon age were used to compare the characteristics of these potential source waters with those of the stream water.

Electric conductivity in steam water differed only slightly between the stations (upstream 0.24mS, downstream 0.25 mS) and pH was 7.4 at both stations. Stream SRP concentration ranged between 29 and 41 µg L^{-1}. SRP contributed 95 % of dissolved (inorganic and organic) P (Tab. 1). The fraction of DO-P was therefore insignificant. In the samples from the groundwater wells and gaining groundwater, SRP concentrations were in the same order of magnitude (12 – 68 µg L^{-1}) and SRP also constituted the dominant fraction of DP (92 ± 15 %, mean ± SD). Low Fe and NH$_4^+$ concentrations in groundwater indicate oxidized groundwater conditions (see Table 1). Sediment pore-water concentrations differed substantially between stations. At the outlet, an elevated SRP pore water concentration exceeding 600 µg L^{-1} was recorded, whereas other P fractions were insignificant. At the upstream station, low sediment pore-water levels of SRP (22 µg L^{-1}) similar to those in the stream were found, but the dissolved P concentration (312 µg L^{-1}) was more than tenfold higher. The SRP/DOP ratio in the sediment was 0.078 and that in stream water 0.935. It is unlikely that turnover in the stream with such a short travel time reverses the ratio of sediment-borne P. It could therefore be concluded that the sediment in the upper part of the stream was unlikely to be a significant source of stream P.

At the outlet concentrations of Fe, DOC, dissolved P and NH$_4^+$ were higher in the sediment pore water than those in the stream (Tab. 1), indicating iron–reductive conditions and the anaerobic decomposition of organic matter. At both stations, the

accumulation of Fe, dissolved P and NH_4^+ in the sediment was consistent with only diffusive and quantitatively-insignificant fluxes of pore-water solutes to the stream.

Table 1: Concentration of SRP, DP, Fe, DOC, NH_4^+ and $\Delta^{14}C$-DOC at upstream and downstream stations (outlet) in different stream compartments and in groundwater wells, sampling campaign Sep. 2020

Compartment	Station	SRP [mg L^{-1}]	DP [mg L^{-1}]	Fe [mg L^{-1}]	DOC [mg L^{-1}]	NH_4^+ [mg L^{-1}]	$\Delta^{14}C$ [‰]
Stream	upper	0.029	0.031	0.159	2.05	0.06	127±4
	outlet	0.041	0.040	0.027	2.48	0.05	-178±3
Sediment pore water	upper	0.022	0.312	2.880	5.46	0.13	-
	outlet	0.654	0.630	26.40	9.12	3.55	-
Streambed sediment leachate	upper	-	-	-	-	-	72±4
	outlet	-	-	-	-	-	6±5
Gaining groundwater	upper	0.040	0.039	0.805	1.33	0.04	-246±3
Groundwater wells, mean values	n=6	0.038	0.043	0.611	1.20	0.119	-

In the stream water, DOC radiocarbon differed dramatically between the two sampled stations. At the upper station, the DOC was enriched in radiocarbon ($\Delta^{14}C$ 127 ‰), meaning that the organic carbon was young, containing carbon that had been fixed photosynthetically after 1950. At the outlet, by contrast, stream water DOC exhibited a negative $\Delta^{14}C$ of -178 ‰, corresponding to a conventional radiocarbon age (CRA) of 1500 years B.P. This signature was much closer to the gaining groundwater DOC (-246 ‰, CRA 2200 years B.P.) than to the DOC signature for the upper station. However, in experiments performed on incubated streambed sediment samples from both stations, young DOC was seen to be released ($\Delta^{14}C$ 6 to 72 ‰).

Our analysis reveals that the SRP-concentrations, DP, and DOC radiocarbon age of the stream water at the outlet compare most closely to the groundwater entering the stream in the upper stream section. Sediment pore water quality differed from that of the gaining groundwater and stream water, with much higher DP, NH_4^+ and DOC concentrations. Thus, gaining groundwater did not interact significantly with the streambed pore water and was probably transported by preferential flow paths. It is known that a fine-grained streambed with low hydraulic conductivity favours preferential flow paths so that largest part of incoming groundwater flux is channelled to a few distinct locations (Schmidt et al. 2006). Sediment pore water, in particular that sampled at the outlet, exhibited high concentrations of DP, Fe and NH_4^+ but low concentrations of NO_3^- along with young DOC radiocarbon ages, suggesting that reductive conditions predominate for mobilization of iron and DP (Smolders et al. 2017). This indicates that sediment was a source of P to the stream, but that transport was quantitatively limited and likely of diffusive and not advective nature only. However, there was no further interaction between the stream water and the sediment pore water at downstream points along the investigation site, instead, the stream water retained the signature introduced in the upstream section by the gaining groundwater. We should note that the stream water sampled at the upper

station showed no signature from the gaining groundwater. The young radiocarbon age of the stream DOC suggests that its source lies in shallow sediments rich in organic material such as riparian soils. In contrast, the presence of aged DOC in groundwater, here with a radiocarbon age of more than 2000 years, is typical of low flow periods (Schiff et al. 1997, Tittel et al. 2022). The groundwater itself needs not be that old, the DOC may have been dissolved and mobilized recently by hydrolysis of old organic carbon from the soil. The limited influence of shallow porewater in the upstream, strongly gaining section is based on the different P speciation in porewater compared to the one observed in the stream water downstream of that section. The limited influence of the streambed SRP sources is supported by i) distinct water and SRP flux gaining in the upstream section but not in the downstream section, ii) hydrochemical similarity of stream water and gaining groundwater, and iii) hydrochemical dissimilarity of sediment pore water and stream water. This finding is in line with the groundwater fraction indicated by the radon data. The radiocarbon results, in combination with the salt tracer and radon data, suggest that gaining groundwater was the principal source of water and solutes entering the stream, particularly under summer low flow conditions.

3.5 Integrating the current observations with SRP measurements from previous studies and into seasonal variability

The long history of studies on water quality in the Schäfertal catchment (see Ollesch 2008) allows us to situate the results of the three sampling campaigns in the wider context of variability in seasonal and discharge dependent SRP concentration. Additionally, earlier work allows comparison with tile drainage water SRP concentrations, which may play a role under high flow conditions.

Stream water observations from previous assessments cover the years 1999 to 2010. We should note that within this time series data there is a small but significant increasing trend in SRP stream water concentrations (Mann-Kendall test, average increase 0.65 µg L^{-1} a^{-1}). Concentrations (Figure 7) are comparable to the measurements carried out for this study. Mean groundwater SRP concentrations in previous assessments of 0.072 mg P L^{-1} (Figure 7) were higher than those sampled in September 2020. The number of wells sampled in past studies was higher than the six wells lying close to the stream that were the focus of the September campaign. When the average SRP concentrations (34.1 µg P L^{-1}) were examined for these six wells only, a good match was revealed with the results obtained in the present study. Water samples from tile drains in 1999 and 2004 showed somewhat low SRP concentrations (0.011 mg P L^{-1}) with a low temporal variability (Std. dev. of 0.006 mg P L-1) (Figure 7). Most of the drainage samples (73%) were taken under colder high flow conditions between January and May.

Stream SRP concentrations displayed clear seasonality, with the highest concentrations occurring under summer low-flow conditions. The resultant concentration-discharge relationship (C = a Q^b) yields an exponent b of -0. 24 (SE 0.045) and thus indicates a mild dilution pattern (Figure 7). The three sampling campaigns in this study capture the typical range of discharge conditions and associated SRP concentrations (Figure 7) very well. The observed mild dilution pattern is in a good agreement with an assessment of concentration dynamics of dissolved PO$_4^+$ in over 700 catchments across Germany: Ebeling et al. (2021) state a mean exponent b of -0.22 and a dominance of dilution patterns in German catchments.
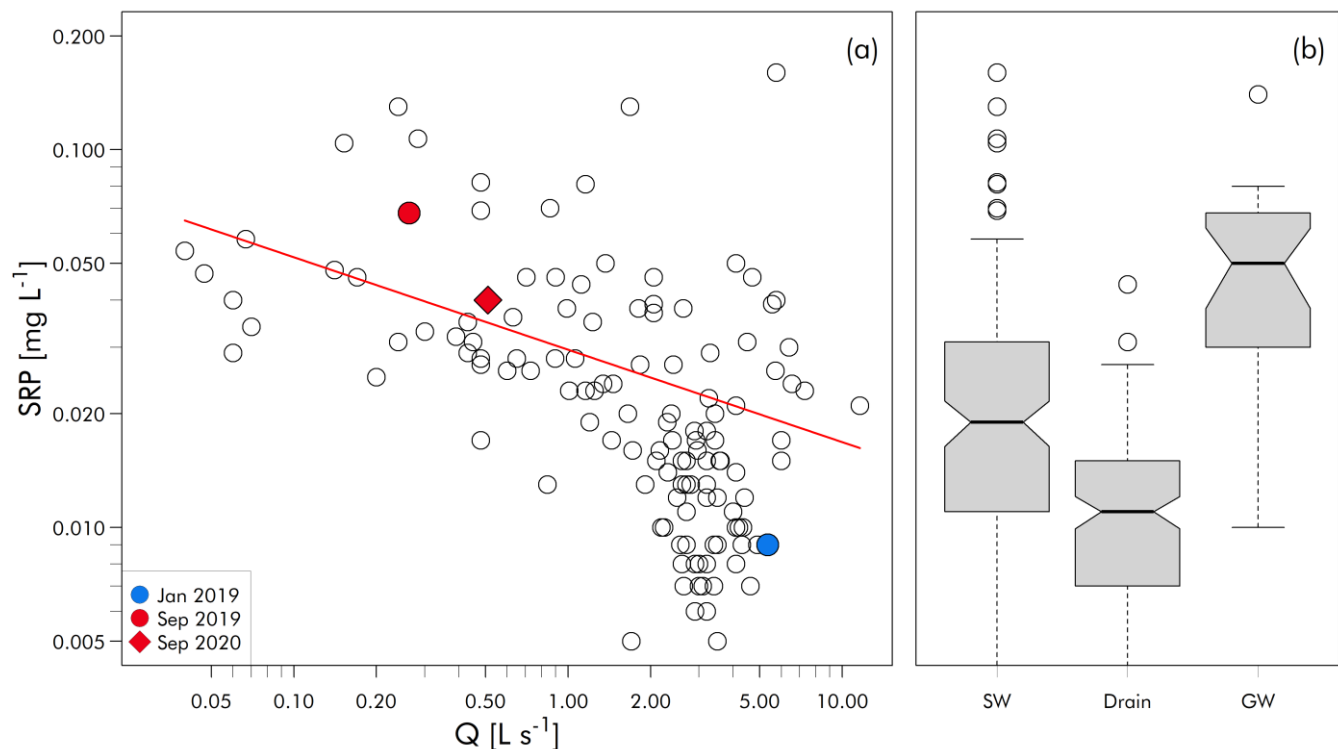
Figure 7: Long-term distribution of concentration discharge relationships for stream SRP at the catchment outlet (left), and box-whisker plots of concentrations in stream water (SW, n=146), tile drains (Drain, n=138), and groundwater (GW, n=25) (right).

When the results of the present SRP source evaluation and longer-term observations of stream water, groundwater and drainage water are taken together, there is strong evidence that groundwater inflow into the stream is the major contributor of SRP in the Schäfertal catchment. This inflow dominates exported concentrations under the summer low-flow conditions, with stream and groundwater concentrations in the same range. Under higher flow conditions other, younger, water components dilute the broadly constant groundwater inputs. While there is evidence for reductive mobilization of SRP within the streambed-sediment pore water, this source does not contribute significantly to exported SRP. The seasonality of SRP concentration is thus not predominantly driven by biogeochemical mediation.

Our findings show that groundwater was the major source of elevated SRP concentrations during summer low-flow conditions. Due to oxidised groundwater conditions, redox processes did not affect SRP fluxes to the stream to any great extent. The observed seasonal differences in SRP levels in the stream water are caused by the seasonally-variable proportion of groundwater to total stream discharge and SRP levels are therefore highest when groundwater dominates stream discharge under summer low-flow conditions. This dominance of groundwater P in stream water P during low-flow periods was also recorded by Jarvie et al. (2008) in UK rural catchments. It also matches the dilution patterns of dissolved P observed in

German catchments (Ebeling et al. 2021). Although groundwater SRP concentrations are moderate in our study, they are well above the critical surface-water threshold for eutrophication of 0.02 to 0.03 mg P L^{-1} (Corell, 1998, King et al. 2014). These findings apply only to typical hard-rock mountain ranges, and groundwater concentrations may differ in other geological settings. Geogenic SRP concentrations can reach even higher levels where organic-matter content is higher or redox processes are more prevalent in the subsurface, as is typically the case for peatlands. The high mobilization of P under reducing conditions may increase its bioavailability, however, it may also increase its loss from soils, particularly in the toe-slope profile (Shaheen et al. 2021).

Interestingly, we could not find clear evidence that intensive arable land use within the catchment was the cause of the elevated SRP concentrations during low flow. Nitrates leaching from soil can be assumed to be an indicator of fertilizer application. In the present study site, these concentrations were high and behaved very differently from SRP concentrations. This can be seen as an indication that the leaching of SRP from soils via seepage water is not the dominant transport mechanism. This finding is in line with the low SRP concentrations observed in the tile drain water (Ollesch 2008). It also agrees with a comprehensive lysimeter study of SRP losses due to agricultural land use, in which arable land exhibited the lowest levels of SRP leaching with mean values of 0.027 mg L-1, while intensive grassland was shown to have SRP concentrations up to five times higher, with a commensurate potential for high SRP loss from soils (Rupp et al. 2018). In addition, the study catchment showed low levels of organic fertilizer (manure) application which, under certain conditions, can increase SRP losses to streams (McDowell et al. 2005, King et al. 2014). One very important factor is the dominance of loamy soils in the study catchment, since such soils display low susceptibility to the preferential flows that can be critical for subsurface SRP losses (Stamm 1998, Simard et al. 2000). The loamy soils in the study catchment show a distinct reduction in TP and in C$_{org}$ –concentration with increasing soil depth. In a typical agricultural soil of the study catchment, TP concentrations were elevated in the A$_p$ horizon (778 mg kg^{-1}) but showed a dramatic drop to a mean value of 193 mg kg^{-1} in the B and C horizon below the plough pan in 40 cm depth, indicating a very high P sorption capacity of the soil. This indicate that P does not leach from the A$_p$ horizon to deeper layers in the investigated soil (Kistner 2007). In contrast to sandy or organic soils (Leinweber et al. 1999)fine textured soils have a reduced potential for P leaching unless there are high P accumulations in the soil (Reid et al. 2012). Our findings confirm the general understanding that SRP concentration in the unsaturated zone is controlled by sorption equilibrium under oxidizing conditions in the upper groundwater, and that SRP losses through seepage are largely buffered (Wriedt et al. 2019). The SRP concentrations found in the gaining groundwater (0.05 mg P L^{-1}, Figure 7) were slightly above mean background concentrations of groundwater from Paleozoic greywacke and Devonian shale of 0.03 mg P L^{-1} but still within the observed range of 0.01 to 0.10 P L^{-1} (Wriedt et al. 2019). The study of Wriedt et al. (2019) did not reveal differences in groundwater SRP concentrations between land use types (arable land, grassland and forest) for these geological units. Although our analyses show that soil leaching of SRP in the study catchment is not very likely, we cannot completely rule out SRP leaching from agricultural soils to groundwater due to slightly higher mean given SRP concentrations in groundwater compared to geological background values. Furthermore, we show that P release from stream sediments was not a major source of stream water P concentration. This finding is consistent with the results of the review by Simpson et al. (2021) who found that on average

480 there was a negative net phosphate exchange potential, meaning that sediments predominantly have a potential to remove P from the water column. In general, stream sediments often have potential to exchange P with the water column and can buffer (retain or release) SRP (Houser 2003, Whiters and Jarvie, 2008, Weiglhofer et al. 2017, Simpson et al. 2021). Recent findings suggest that stream sediments can act as a source when P loading is elevated, the SRP/Fe relationship is high and DO concentrations are low (van Deal et al 2021a). Although we found anoxic conditions in stream sediments, rates of diffusive

485 transport were too low to release any considerable quantity of P into the stream water. More significant P releases from stream sediments have been found in slow-flowing lowland streams with considerable legacy P from point source inputs (van Deal et al. 2020). Such experimental evidence of P release from stream sediments is still rare, but new modelling approaches may help to assess potential P losses from stream sediments to the water column (van Deal et al. 2021b).

4 Conclusions

490 The results of this study indicate that groundwater was the major source of stream water P during ecologically-relevant low-flow conditions. Furthermore, agricultural land use did not result in high levels of P loading in the stream during low-flow conditions. Low potential P fluxes from stream sediments further suggest that the elevated particulate P concentration in agricultural topsoils delivered to the stream by individual soil-erosion events also observed in former studies did not yield significant SRP releases from stream sediment in the study catchment. Nevertheless, stream SRP concentrations during

495 summer low flow were well above the critical threshold for eutrophication and were hence sufficient to cause environmental degradation. Although, in the study catchment, it is unlikely that stream sediments originating from arable land raised stream SRP concentrations considerably during low flow, the prevention of soil erosion may reduce the downstream transport of sediments with high P loads and the further release of SRP into stagnant waters. Efforts to reduce stream eutrophication and enhance primary production during sensitive low flow periods should focus on decreasing the availability of light and reducing

500 stream temperature through the re-introduction of more riparian vegetation. Currently enriched P in agricultural soils (Schachtschabel et al. 1992, Pöthig et al. 2010) is still a potential long-term P source for surface waters. Under certain conditions, this legacy P can be transported from soils to surface waters by surface runoff and soil erosion, as well as by leaching from soils (e.g. Rowe et al. 2016, McCrackin et al. 2018). Therefore, control measures for reducing agricultural P effect on surface waters should always be based on carefully identified P-sources in a given catchment.

505 **Acknowledgments**

We thank our colleagues at Helmholtz-Centre for Environmental Research (UFZ) for valuable discussions at the early stage of this study. We thank the UFZ Analytics Department (GEWANA) for performing the chemical analysis of the collected samples. We also thank the technicians at UFZ Magdeburg and UFZ Halle for their continuous efforts to maintain the monitoring activities at the Schäfertal. We thank Xiaoqiang Yang for support of figure preparation. We thank Gregor

510 Ollesch for providing the long term SRP data. The monitoring equipment was partly funded by TERENO (www.tereno.net), financed by the German Federal Ministry of Education and Research (BMBF).

Data availability

Long term hydrological data sets have been published in Supplement of Yang et al. 2021. The long term SRP dataset used in this study will be available upon request to the corresponding author.

515 **Author contribution**

MR: conceptualization, methodology, formal analysis, investigation, writing- original draft preparation, visualization. JT: conceptualization, methodology, formal analysis, investigation, writing- original draft preparation. FR: investigation, writing- reviewing and editing, visualization. MS: investigation, writing- reviewing and editing, visualization. KK: methodology, investigation, reviewing and editing. BG: software, validation, visualization. FM: investigation, visualization, reviewing and editing. AM: conceptualization, methodology, formal analysis, investigation, writing- original draft preparation, visualization.

Competing interests

The authors declare that they have no conflict of interest.

References

Anis, M. R. and Rode, M.: Effect of climate change on overland flow generation: a case study in central Germany, Hydrological 525 Processes, 29, 2478-2490, 2015.

Bechmann, M., Deelstra, J., Stalnacke, P., Eggestad, H. O., Oygarden, L., and Pengerud, A.: Monitoring catchment scale agricultural pollution in Norway: policy instruments, implementation of mitigation methods and trends in nutrient and sediment losses, Environmental Science & Policy, 11, 102-114, 2008.

Behrendt, H. and Boekhold, A.: PHOSPHORUS SATURATION IN SOILS AND GROUNDWATERS, Land Degradation 530 and Rehabilitation, 4, 233-243, 1993.

Bernal, S., Lupon, A., Ribot, M., Sabater, F., and Marti, E.: Riparian and in-stream controls on nutrient concentrations and fluxes in a headwater forested stream, Biogeosciences, 12, 1941-1954, 2015.

Bol, R., Gruau, G., Mellander, P. E., Dupas, R., Bechmann, M., Skarbovik, E., Bieroza, M., Djodjic, F., Glendell, M., Jordan, P., Van der Grift, B., Rode, M., Smolders, E., Verbeeck, M., Gu, S., Klumpp, E., Pohle, I., Fresne, M., and Gascuel-Odoux, 535 C.: Challenges of Reducing Phosphorus Based Water Eutrophication in the Agricultural Landscapes of Northwest Europe, Frontiers in Marine Science, 5, 2018.

Bormann, F. H. and Likens, G. E.: NUTRIENT CYCLING, Science, 155, 424-+, 1967.

Brookfield, A. E., Hansen, A. T., Sullivan, P. L., Czuba, J. A., Kirk, M. F., Li, L., Newcomer, M. E., and Wilkinson, G.: Predicting algal blooms: Are we overlooking groundwater?, Science of the Total Environment, 769, 2021.

540   Chardon, W. J., Aalderink, G. H., and van der Salm, C.: Phosphorus leaching from cow manure patches on soil columns, Journal of Environmental Quality, 36, 17-22, 2007.

Correll, D. L.: The role of phosphorus in the eutrophication of receiving waters: A review, Journal of Environmental Quality, 27, 261-266, 1998.

Cornell, R.M., Schwertmann, U.: The Iron Oxides: Structure, Properties, Reactions, Occurences and Uses. 2nd ed. Wiley-
545   VCH Verlag GmbH & Co. 2003.

Dils, R. M. and Heathwaite, A. L.: The controversial role of tile drainage in phosphorus export from agricultural land, Water Science and Technology, 39, 55-61, 1999.

DIN EN ISO 6878: Water quality determination of Phosphorus-ammonium molybdate spectrometric method. Beuth, Berlin. 2004.

550   Dupas, R., Mellander, P. E., Gascuel-Odoux, C., Fovet, O., McAleer, E. B., McDonald, N. T., Shore, M., and Jordan, P.: The role of mobilisation and delivery processes on contrasting dissolved nitrogen and phosphorus exports in groundwater fed catchments, Science of the Total Environment, 599, 1275-1287, 2017.

Dupas, R., Tittel, J., Jordan, P., Musolff, A., and Rode, M.: Non-domestic phosphorus release in rivers during low-flow: Mechanisms and implications for sources identification, Journal of Hydrology, 560, 141-149, 2018.

555   Ebeling P, Kumar R, Weber M, Knoll L, Fleckenstein JH, Musolff A:. Archetypes and controls of riverine nutrient export across German catchments. Water Resources Research, 57(4). doi:10.1029/2020WR028134, 2021.

Frei, S. and Gilfedder, B. S.: FINIFLUX: An implicit finite element model for quantification of groundwater fluxes and hyporheic exchange in streams and rivers using radon, Water Resources Research, 51, 6776-6786, 2015.

Genereux, D. P. and Hemond, H. F.: DETERMINATION OF GAS-EXCHANGE RATE CONSTANTS FOR A SMALL
560   STREAM ON WALKER BRANCH WATERSHED, TENNESSEE, Water Resources Research, 28, 2365-2374, 1992.

Graeff, T., Zehe, E., Reusser, D., Luck, E., Schroder, B., Wenk, G., John, H., and Bronstert, A.: Process identification through rejection of model structures in a mid-mountainous rural catchment: observations of rainfall-runoff response, geophysical conditions and model inter-comparison, Hydrological Processes, 23, 702-718, 2009.

Gu, S., Gruau, G., Dupas, R., Rumpel, C., Creme, A., Fovet, O., Gascuel-Odoux, C., Jeanneau, L., Humbert, G., and Petitjean,
565   P.: Release of dissolved phosphorus from riparian wetlands: Evidence for complex interactions among hydroclimate variability, topography and soil properties, Science of the Total Environment, 598, 421-431, 2017.

Haygarth, P. M., Jarvie, H. P., Powers, S. M., Sharpley, A. N., Elser, J. J., Shen, J. B., Peterson, H. M., Chan, N. I., Howden, N. J. K., Burt, T., Worrall, F., Zhang, F. S., and Liu, X. J.: Sustainable Phosphorus Management and the Need for a Long-Term Perspective: The Legacy Hypothesis, Environmental Science & Technology, 48, 8417-8419, 2014.

570   Heathwaite, A. L. and Dils, R. M.: Characterising phosphorus loss in surface and subsurface hydrological pathways, Science of the Total Environment, 251, 523-538, 2000.

Heckrath, G., Brookes, P. C., Poulton, P. R., and Goulding, K. W. T.: PHOSPHORUS LEACHING FROM SOILS CONTAINING DIFFERENT PHOSPHORUS CONCENTRATIONS IN THE BROADBALK EXPERIMENT, Journal of Environmental Quality, 24, 904-910, 1995.

575   House, W. A.: Geochemical cycling of phosphorus in rivers, Applied Geochemistry, 18, 739-748, 2003.

Jarvie, H. P., Haygarth, P. M., Neal, C., Butler, P., Smith, B., Naden, P. S., Joynes, A., Neal, M., Wickham, H., Armstrong, L., Harman, S., and Palmer-Felgate, E. J.: Stream water chemistry and quality along an upland-lowland rural land-use continuum, south west England, Journal of Hydrology, 350, 215-231, 2008.

Jeanneau, L., Jaffrezic, A., Pierson-Wickmann, A. C., Gruau, G., Lambert, T., and Petitjean, P.: Constraints on the Sources
580   and Production Mechanisms of Dissolved Organic Matter in Soils from Molecular Biomarkers, Vadose Zone Journal, 13, 2014.

King, S. A., Heffernan, J. B., and Cohen, M. J.: Nutrient flux, uptake, and autotrophic limitation in streams and rivers, Freshwater Science, 33, 85-98, 2014.

Kistner, I., Ollesch, G., Meissner, R., and Rode, M.: Spatial-temporal dynamics of water soluble phosphorus in the topsoil of
585   a low mountain range catchment, Agriculture Ecosystems & Environment, 176, 24-38, 2013.

Kistner, I., 2007: Anwendung des Modells ANIMO zur Simualtion des gelösten Phosphors im Oberflächenabfluss auf der Feldskala und der Phosphorverfügbarkeit im Oberboden auf der Einzugsgebietsskala (in German). Dissertation, Martin Lutter University Halle,182 p.

Kleinman, P. J. A., Needelman, B. A., Sharpley, A. N., and McDowell, R. W.: Using soil phosphorus profile data to assess
590   phosphorus leaching potential in manured soils, Soil Science Society of America Journal, 67, 215-224, 2003.

Kleinman, P. J. A., Sharpley, A. N., Saporito, L. S., Buda, A. R., and Bryant, R. B.: Application of manure to no-till soils: phosphorus losses by sub-surface and surface pathways, Nutrient Cycling in Agroecosystems, 84, 215-227, 2009.

Kleinman, P. J. A., Sharpley, A. N., Saporito, L. S., Buda, A. R., and Bryant, R. B.: Application of manure to no-till soils: phosphorus losses by sub-surface and surface pathways, Nutrient Cycling in Agroecosystems, 84, 215-227, 2009.

595   Knorr, K. H.: DOC-dynamics in a small headwater catchment as driven by redox fluctuations and hydrological flow paths - are DOC exports mediated by iron reduction/oxidation cycles? Biogeosciences, 10, 891-904, 2013.

Leinweber, P., Meissner, R., Eckhardt, K. U., and Seeger, J.: Management effects on forms of phosphorus in soil and leaching losses, European Journal of Soil Science, 50, 413-424, 1999.

Little, J. L., Nolan, S. C., Casson, J. P., and Olson, B. M.: Relationships between soil and runoff phosphorus in small Alberta
600   watersheds, Journal of Environmental Quality, 36, 1289-1300, 2007.

McDowell, R. W., Condron, L. M., Stewart, I., and Cave, V.: Chemical nature and diversity of phosphorus in New Zealand pasture soils using P-31 nuclear magnetic resonance spectroscopy and sequential fractionation, Nutrient Cycling in Agroecosystems, 72, 241-254, 2005.

McDowell, R. W. and Sharpley, A. N.: Approximating phosphorus release from soils to surface runoff and subsurface drainage,
605   Journal of Environmental Quality, 30, 508-520, 2001.

Moncelon, R., Gouaze, M., Pineau, P., Beneteau, E., Breret, M., Philippine, O., Robin, F. X., Dupuy, C., and Metzger, E.: Coupling between sediment biogeochemistry and phytoplankton development in a temperate freshwater marsh (Charente-Maritime, France): Evidence of temporal pattern, Water Research, 189, 2021.

Musolff, A., Selle, B., Bttner, O., Opitz, M., and Tittel, J.: Unexpected release of phosphate and organic carbon to streams linked to declining nitrogen depositions, Global Change Biology, 23, 1891-1901, 2017.

Ollesch, G.: Measuring and modeling of snowmelt erosion using the example of headwater catchments Schäfertal (Germany) and Lubazhinkha (Russia) (in German). Habilitation, Faculty of Geosciences, Geoengineering and Mining, TU Bergakademie Freiberg, Freiberg, Germany, 213p., 2008.

Ollesch, G., Sukhanovski, Y., Kistner, I., Rode, M., and Meissner, R.: Characterization and modelling of the spatial heterogeneity of snowmelt erosion, Earth Surface Processes and Landforms, 30, 197-211, 2005.

Payn, R. A., Gooseff, M. N., McGlynn, B. L., Bencala, K. E., and Wondzell, S. M.: Channel water balance and exchange with subsurface flow along a mountain headwater stream in Montana, United States, Water Resources Research, 45, 2009.

Petermann, E., Knoller, K., Rocha, C., Scholten, J., Stollberg, R., Weiss, H., and Schubert, M.: Coupling End-Member Mixing Analysis and Isotope Mass Balancing (222-Rn) for Differentiation of Fresh and Recirculated Submarine Groundwater Discharge Into Knysna Estuary, South Africa, Journal of Geophysical Research-Oceans, 123, 952-970, 2018.

Pöthig, R., Behrendt, H., Opitz, D., Furrer, G., 2010. A universal method to assess the potential of phosphorus loss from soil to aquatic ecosystems. Environ. Sci. Pollut.Res. 17, 497–504.

Raymond PA, Zappa CJ, Butman D, et al (2012) Scaling the gas transfer velocity and hydraulic geometry in streams and small rivers. Limnology and Oceanography: Fluids and Environments 2:41–53.

Reid, D. K., Ball, B., and Zhang, T. Q.: Accounting for the Risks of Phosphorus Losses through Tile Drains in a Phosphorus Index, Journal of Environmental Quality, 41, 1720-1729, 2012.

Rode, M., Wade, A. J., Cohen, M. J., Hensley, R. T., Bowes, M. J., Kirchner, J. W., Arhonditsis, G. B., Jordan, P., Kronvang, B., Halliday, S. J., Skeffington, R. A., Rozemeijer, J. C., Aubert, A. H., Rinke, K., and Jomaa, S.: Sensors in the Stream: The High-Frequency Wave of the Present, Environmental Science & Technology, 50, 10297-10307, 2016.

Rupp, H., Meissner, R., and Leinweber, P.: Plant available phosphorus in soil as predictor for the leaching potential: Insights from long-term lysimeter studies, Ambio, 47, 103-113, 2018.

Scheffer, F. 1992: Lehrbuch der Bodenkunde/ Scheffer Schachtschabel.13. Auflage, Stuttgart: Enke Verlag, 491 p.

Schiff S.L., Aravena R., Trumbore S.E., Hinton M.J., Elgood R., Dillon P.J.: Export of DOC from forested catchments on the Precambrian Shield of Central Ontario: Clues from 13C and 14C. Biogeochemistry 36:43–65, 1997.

Schmidt, C., Bayer-Raich, M., Schirmer, M.: Characterization of spatial heterogeneity of groundwater-stream water interactions using multiple depth streambed temperature measurements at the reach scale. Hydrol. Earth Syst. Sci. 10 (6), 849 – 859, 2006.

Schron, M., Kohli, M., Scheiffele, L., Iwema, J., Bogena, H. R., Lv, L., Martini, E., Baroni, G., Rosolem, R., Weimar, J., Mai, J., Cuntz, M., Rebmann, C., Oswald, S. E., Dietrich, P., Schmidt, U., and Zacharias, S.: Improving calibration and validation of cosmic-ray neutron sensors in the light of spatial sensitivity, Hydrology and Earth System Sciences, 21, 5009-5030, 2017.

Schubert, M., Buerkin, W., Pena, P., Lopez, A. E., and Balcazar, M.: On-site determination of the radon concentration in water samples: Methodical background and results from laboratory studies and a field-scale test, Radiation Measurements, 41, 492-497, 2006.

645   Schubert, M., Knoeller, K., Mueller, C., and Gilfedder, B.: Investigating River Water/Groundwater Interaction along a Rivulet Section by Rn-222 Mass Balancing, Water, 12, 2020.

Shaheen, S. M., Wang, J. X., Baumann, K., Wang, S. L., Leinweber, P., and Rinklebe, J.: Redox-induced mobilization of phosphorus in groundwater affected arable soil profiles, Chemosphere, 275, 2021.

Simard, R. R., Beauchemin, S., and Haygarth, P. M.: Potential for preferential pathways of phosphorus transport, Journal of Environmental Quality, 29, 97-105, 2000.

650   Simard, R. R., Beauchemin, S., and Haygarth, P. M.: Potential for preferential pathways of phosphorus transport, Journal of Environmental Quality, 29, 97-105, 2000.

Simpson, Z. P., McDowell, R. W., Condron, L. M., McDaniel, M. D., Jarvie, H. P., and Abell, J. M.: Sediment phosphorus buffering in streams at baseflow: A meta-analysis, Journal of Environmental Quality, 50, 287-311, 2021.

Smolders, E., Baetens, E., Verbeeck, M., Nawara, S., Diels, J., Verdievel, M., Peeters, B., De Cooman, W., and Bakens, S.:
655   Internal Loading and Redox Cycling of Sediment Iron Explain Reactive Phosphorus Concentrations in Lowland Rivers, Environmental Science & Technology, 51, 2584-2592, 2017.

Stamm, C., Fluhler, H., Gachter, R., Leuenberger, J., and Wunderli, H.: Preferential transport of phosphorus in drained grassland soils, Journal of Environmental Quality, 27, 515-522, 1998.

Stuiver, M. and Polach, H. A.: Discussion Reporting of 14C Data, Radiocarbon, 19, 355-363, 1977.

660   Stuiver, M. and Polach, H. A.: REPORTING OF C-14 DATA - DISCUSSION, Radiocarbon, 19, 355-363, 1977.

Tittel, J., Büttner, O., Freier, K., Heiser, A., Sudbrack, R., and Ollesch, G.: The age of terrestrial carbon export and rainfall intensity in a temperate river headwater system, Biogeochemistry, 115, 53-63, 2013.

Tittel, J., Musolff, A., Rinke, K., Büttner, O.: Anthropogenic transformation disconnects a lowland river from contemporary carbon stores in its catchment. Ecosystems 25: 618-632, 2022.

665   Tittel, J., Büttner, O., Friese, K., Lechtenfeld, O. J., Schuth, S., von Tümpling, W., and Musolff, A.: Iron Exports From Catchments Are Constrained by Redox Status and Topography, Global Biogeochemical Cycles, 36, e2021GB007056, 2022.

van Dael, T., De Cooman, T., and Smolders, E.: In-stream oxygenation to mitigate internal loading of phosphorus in lowland streams, Journal of Hydrology, 590, 2020.

van Dael, T., De Cooman, T., Verbeeck, M., and Smolders, E.: Sediment respiration contributes to phosphate release in lowland
670   surface waters, Water Research, 168, 2020.

van Dael, T., De Cooman, T., Verbeeck, M., and Smolders, E.: Sediment respiration contributes to phosphate release in lowland surface waters, Water Research, 168, 2020.

Van Dael, T., Xia, L., Van Dijck, K., Potemans, S., and Smolders, E.: Internal loading of phosphate in rivers reduces at higher flow velocity and is re duce d by iron rich sand application: an experimental study in flumes, Water Research, 198, 2021.

675 Withers, P. J. A. and Jarvie, H. P.: Delivery and cycling of phosphorus in rivers: A review, Science of the Total Environment, 400, 379-395, 2008.

Wriedt, G. and Randt, C.: Groundwater phosphate levels in Lower Saxony-Distribution, influence factors and threshold value, Grundwasser, 24, 109-127, 2019.

Yang, J., Heidbuchel, I., Musolff, A., Reinstorf, F., and Fleckenstein, J. H.: Exploring the Dynamics of Transit Times and 680 Subsurface Mixing in a Small Agricultural Catchment, Water Resources Research, 54, 2317-2335, 2018.

Yang, X. Q., Tetzlaff, D., Soulsby, C., Smith, A., and Borchardt, D.: Catchment Functioning Under Prolonged Drought Stress: Tracer-Aided Ecohydrological Modeling in an Intensively Managed Agricultural Catchment, Water Resources Research, 57, 2021.

Zak, D. and Gelbrecht, J.: The mobilisation of phosphorus, organic carbon and ammonium in the initial stage of fen rewetting 685 (a case study from NE Germany), Biogeochemistry, 85, 141-151, 2007.